

Tilted-field radio-frequency size effect in tungsten*

D. R. Baer[†]

Laboratory of Atomic and Solid State Physics, Cornell University, Ithaca, New York 14850

(Received 31 July 1974)

The radio-frequency size effect (RFSE) has been studied in tungsten plates in a magnetic field inclined at an angle to the sample surface using a transmission method. A parametrized model of the tungsten Fermi surface and the geometric model of the RFSE have been combined to allow calculation of expected signal positions. Most of the well-defined experimental signals are identifiable using the model and there is general agreement between the experimental data and the calculated signal locations. The relation of the tilted-field RFSE signals to Gantmakher-Kaner oscillations is also discussed.

INTRODUCTION

The radio-frequency size effect (RFSE) has been used extensively to measure Fermi-surface (FS) dimensions and electron scattering rates in metals. While the experimental RFSE signals may seem very complicated, much of the spectroscopy can be accurately understood in terms of a simple ballistic model of electron motion.^{1,2} Percy *et al.*² have demonstrated this in detail for potassium.

Although such a model is not necessary to understand the signals observed when the magnetic field is oriented parallel to the sample plane, it does give useful insight into those occurring when the field is tilted out of that plane; thus it provides the basis for studies of tilted-field RFSE phenomena in metals with Fermi surfaces more complex than that of potassium. Such signals have been observed in a number of metals, but the complexity of their Fermi surfaces has generally limited detailed study to either small tilt angles or special sections of the FS, and as a result, the ballistic model has not been tested in this situation.

Two experimental RFSE techniques have been used to study temperature-dependent scattering in metals.³ The first measures the temperature dependence of the parallel-field signal amplitude, while the second measures the temperature dependence of the amplitude of limiting-point signals occurring when the magnetic field is tilted out of the sample plane. Because limiting-point electrons make only one pass through each skin depth of the sample before striking its surface and are confined to localized parts of the FS, the second method appears to offer several advantages over the parallel-field method. However, because limiting-point signals are not observable in many metals, and the other more easily observed tilted-field signals offer the same advantages, a study of this aspect of the RFSE promises to be valuable.

Although the FS of tungsten is well known^{4,5} and

the parallel-field RFSE and its temperature dependence have been studied extensively,⁶⁻⁸ there are presently no reported observations of a limiting-point signal in tungsten. In this paper it is demonstrated that most of the complex tilted-field RFSE signals observed in tungsten plates can be understood by combining the parametrized model of the tungsten FS and the ballistic model of the RFSE using a computer. It is also shown that in some situations RFSE signals are produced by the same electrons as those involved in Gantmakher-Kaner oscillations, and that tilted-field signals other than limiting-point signals may be useful for the study of electron scattering anisotropy in tungsten.

RFSE BALLISTIC MODEL, TUNGSTEN FS, AND COMPUTER CALCULATION

The RFSE is a well-known phenomenon⁹ and the procedure used in this paper to predict the location of the signals is essentially the same as that discussed by Percy *et al.*² for potassium. The discussion below will briefly outline some aspects of the ballistic model to establish the notation used throughout the paper, then describe the tungsten FS model and the method used to calculate the RFSE signal locations.

Consider a thin metal plate of thickness D , whose surface normal is in the \hat{z} direction, placed in a dc magnetic field \vec{H} , with an rf electric field oriented parallel to one surface. RFSE signals are observed when a change in H produces a sharp change in the number of electrons whose trajectories have effective points ($v_z = 0$) at both surfaces of the sample. (Signals are also produced, when \vec{H} is parallel to the sample surface, by chains of two or more trajectories which fit in the sample and meet the requirements just described.) The quantity important for prediction of signal locations is the depth d_z that an electron travels into the sample as it moves between effective points on

its \vec{k} -space orbit.

$$d_z = \vec{d} \cdot \hat{z}, \quad (1)$$

where

$$\vec{d} = \int_{t_1}^{t_2} \vec{v} dt = \frac{h}{|e|aH} \int_{k_1}^{k_2} \frac{dk_{\parallel} \vec{v}}{|v_{\perp}|}.$$

k_1 and k_2 refer to effective points on the orbit, h is Planck's constant, a is the lattice constant, and e is the electron charge; \vec{v} is the electron velocity, v_{\perp} is the component perpendicular to \vec{H} , and dk_{\parallel} is an element of arc along the orbit; the wave vector \vec{k} is expressed in units of $2\pi/a$.

For present purposes it is convenient to consider the field-independent product of H and d_z . In a tilted magnetic field, Eq. (1) defines many values of Hd_z corresponding to successive revolutions around the orbit; if the orbit is sufficiently complex with several effective points, a multitude of additional values is introduced. It is customary to label FS orbits by their constant projection of \vec{k} along \vec{H} , which is denoted k_H . Hd_z can then be considered a function of k_H and may be multivalued for situations in which two or more orbits exist with the same value of k_H . According to the ballistic model described in Ref. 2, RFSE signals are produced by orbits with cutoff or extremal [$d(Hd_z)/dk_H = 0$] values of Hd_z , or $(Hd_z)_{\text{ext}}$.¹⁰

For Eq. (1) to be useful, the FS must be known. The tungsten FS, as shown in Fig. 1, consists of an electron jack, a hole octahedron, and six hole ellipsoids. A parameterized model of this FS, fit to de Haas-van Alphen data and referred to as GGP, was first presented by Girvan *et al.*⁴ and has aided in understanding several types of phenomena including the parallel-field RFSE, quantum oscillations in the acoustic attenuation,¹¹ and, with some small revision, Doppler-shifted cyclotron resonance⁵ and Sondheimer magnetomorphic effects.¹²

We have programed the revised model (RGGP) on a PDP 11/20 computer to calculate the electron trajectories as a function of k_H using the following method.¹³ An initial \vec{k} vector with a desired value of k_H is chosen; it is generally not on the FS and must be corrected to lie on it by incrementing appropriately along the component of \vec{v} in the plane of the orbit. The correction is made using Newton's method, and a new \vec{k} lying in the plane of the orbit is computed by incrementing the old \vec{k} by $\Delta\vec{k}$, where $\Delta\vec{k}$ is parallel to the Lorentz force on the electron at \vec{k} . The new \vec{k} is again not on the FS and is corrected as before. The process is repeated until a complete k -space orbit is traced out. Once the k -space orbit is known, the real-space trajectory may be calculated by numerical integration of Eq. (1).

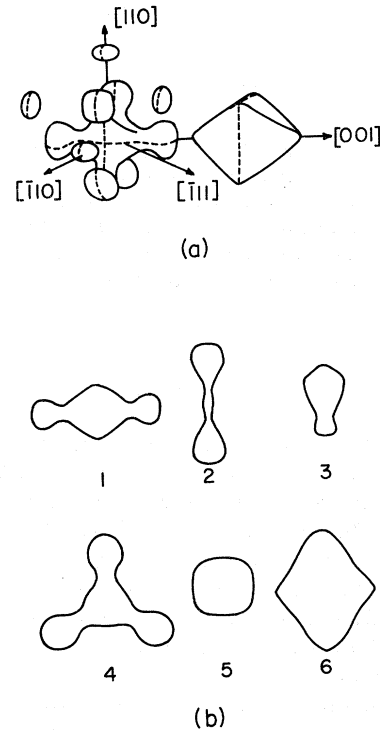


FIG. 1. (a) Drawing of tungsten Fermi surface (after Ref. 12). (b) Examples of orbits formed on tungsten Fermi surface: 1, jack two-ball orbit; 2, different jack two-ball orbit; 3, jack one-ball orbit; 4, jack three-ball orbit; 5, jack isolated one-ball orbit; 6, octahedron orbit.

It is advantageous to plot the projection of the real-space trajectory onto a plane that includes the surface normal (\hat{z}). In this manner the effective points ($\vec{v} \cdot \hat{z} = 0$) are easily identified and all possible Hd_z values can be read directly from the plot. Figure 2 shows the projection of a sample octahedron trajectory onto the yz plane, with the effective points marked and one of the several possible Hd_z values indicated. The magnetic field lies in the plane which includes the $[110]$ surface normal (\hat{z}) and the $[1\bar{1}0]$ \hat{x} direction and is tilted by an angle $\psi = 20^\circ$ out of the plane of the surface. It should be noted that for this particular trajectory there are several pairs of effective points, but that not every pair is viable in the sense that the *entire* trajectory between effective points must lie within the plate.

Figure 3 shows a plot of Hd_z as a function of k_H for the octahedron, when the magnetic field is directed as described above ($\psi = 20^\circ$) and for the parallel-field case ($\psi = 0^\circ$). This graph, obtained from many orbit projections, has several noteworthy aspects. First, as already noted, orbits with extremal or cutoff values of Hd_z should pro-

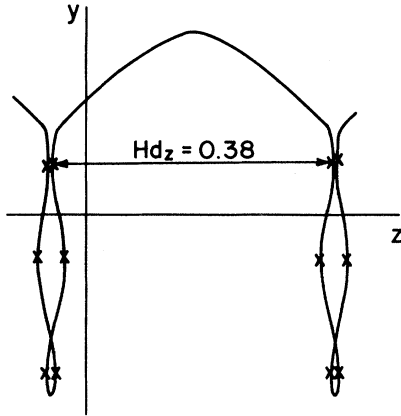


FIG. 2. Projection of a real-space trajectory of an orbit from the tungsten octahedron with effective points marked. $k_H = 0.22$ and $\psi = 20^\circ$ from $[1\bar{1}0]$ toward $[110]$. One of the several possible Hd_z distances for this orbit is marked.

duce the RFSE signals. The extremal orbits are said to be focused because a small change in k_H produces only a second-order change in Hd_z . Second, two curves for $\psi = 20^\circ$ are shown. The lower curve is produced by orbits of less than

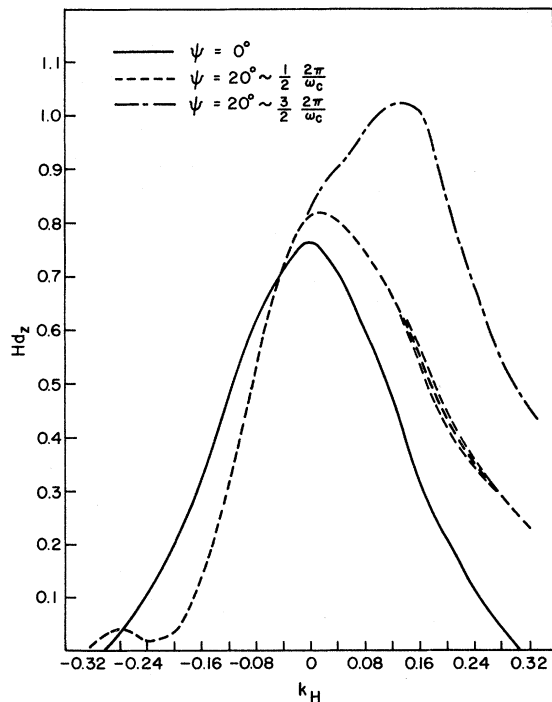


FIG. 3. Hd_z as a function of k_H for the octahedron surface of tungsten at two tilt angles. k_H is in units of $2\pi/a$ ($=1.987 \text{ \AA}^{-1}$) and Hd_z is in units of \hbar/ea ($=130.8 \text{ Gmm}$).

one cyclotron period between effective points, while the second curve gives Hd_z values for effective points roughly $1\frac{1}{2}$ cyclotron periods apart. The two curves produce $(Hd_z)_{\text{ext}}$ at different k_H and the corresponding RFSE signals are therefore produced by different groups of electrons. In general, similar curves can be calculated for orbits of roughly $(2n+1)/2$ cyclotron periods, where $n = 0, 1, 2, \dots$, but the total path length that the electron must travel in going from one surface to the other may become too large to produce an observable signal. (See Refs. 1 and 2 for details.) Third, the $\psi = 20^\circ$ line splits around $k_H = 0.22$ due to the many effective points on the particular trajectory shown in Fig. 2. However, the Hd_z values at this value of k_H are not near $(Hd_z)_{\text{ext}}$ and the details are of little interest. Finally, the general shape of the Hd_z curve for the octahedron is similar to that for a sphere² in that both curves have extremal and cutoff values of Hd_z .

Consideration of the electron-jack section of the FS adds several complications both because k_H often does not define a unique orbit on the FS and because of the large number of effective points on some of the complex trajectories. Figure 4 shows a plot of Hd_z for the jack portion of the FS when the magnetic field is directed as for Figs. 2 and 3. The intricacy of the jack shape seems to allow very few extremal values of Hd_z .

The ellipsoid parts of the FS have not yet been included in these calculations because the most easily observed RFSE signals can readily be explained without them.

The computer calculations have been checked for systematic errors in two ways. To test the accuracy of programming the GGP and RGGP FS models, the areas of several orbits were calculated and the extremal values of the areas were compared with published results. Because of the allowed step size and the required convergence to the FS, the calculations were expected to be accurate to about 1%, and in fact agree with the published values to better than 2%, which is satisfactory for our purposes. As a second check on the method of calculation, a spherical FS was programmed in the same manner as that used for the RGGP model and the resulting values of Hd_z were compared to the analytic expression derived in Ref. 2. There was no observable difference between the results of the two methods of calculation.

In order to explore the effects of slight changes in the FS model on the computer calculations, some calculations have been performed using both the GGP and RGGP models. The changes in the model cause some changes in the jack calculations, but the trends are essentially the same. Some parts of the electron trajectories depend upon the

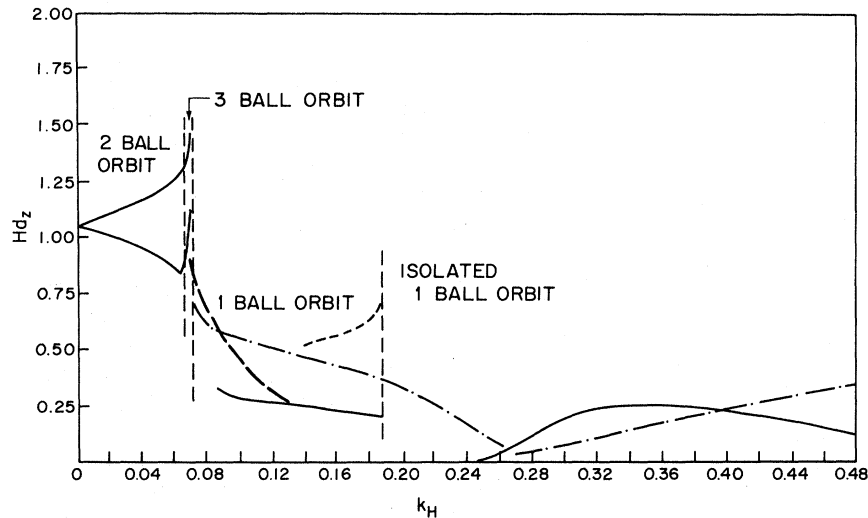


FIG. 4. Hd_z as a function of k_H for the jack surface of tungsten. $\psi = 20^\circ$ from $[1\bar{1}0]$ toward $[110]$.

general shape of the FS while other parts may depend upon the detailed FS shape near a corner or turning point; therefore some disagreement between the calculations and the experimental results may be expected even if the over-all agreement is quite good.

EXPERIMENTAL DETAILS

The experiments were performed in a superconducting omnidirectional magnet system¹⁴ using a transmission method that has been discussed elsewhere.¹⁵ Spiral generator and receiver coils, which allow transmission and detection of all polarizations of the rf field, were used at rf frequencies of 1.25 and 10.0 MHz. The static magnetic field was modulated at 4 Hz.

The single-crystal tungsten plates, which are roughly 1 cm in diameter and about 0.4 mm thick, were cut from a zone-refined rod and then electro-polished. The sample thickness, as measured by a micrometer, is consistent with the observation of the known parallel-field RFSE signals. The alignment of the sample in the magnetic field was judged to be within 2° of the stated values and this degree of error has been observed not to be critical for most orientations.

COMPARISON OF EXPERIMENTAL RESULTS AND CALCULATIONS

When \vec{H} is directed in a plane parallel to the sample surface, the RFSE signals correspond to extremal caliper dimensions of the FS. The top curve in Fig. 5 shows the field derivative of the rf transmission through the sample as a function of magnetic field, for a tungsten plate whose surface normal is in the $[110]$ direction, with \vec{H}

oriented along the $[1\bar{1}0]$ direction in the sample plane. The signal at roughly 270 G originates from the hole octahedron, while the 85- and 400-G signals originate from one- and two-ball jack orbits, respectively. When the magnetic field is tilted out of the plane of the surface, the location of a signal depends upon the details of the three-dimensional electron trajectories. The additional curves in Fig. 5 show the signal observed for different tilt angles ψ as the magnetic field is rotated from the $[1\bar{1}0]$ direction toward the $[110]$ sample normal. The evolution of the signals as the field is tilted can be followed by careful examination of Fig. 5. The low-field jack signal is observable over a range of field angles with very little change, and even appears at large tilt angles in a washed-out manner. The hole octahedron signal moves to higher fields as the field is tilted and reaches a maximum amplitude at approximately $\psi = 50^\circ$. This maximum may be explained in two ways. First, relative to the group of electrons producing the $\psi = 0$ signal, the focused electrons at $\psi = 50^\circ$ travel parallel to the surface of the metal for a longer time, thereby acquiring larger amounts of energy from the rf field. Second, because there are several neighboring effective points on the $\psi = 50^\circ$ focused orbits, there are several slightly different groups of electrons that happen to be focused at nearly the same value of Hd_z , allowing a large number of electrons to participate in the signal. The 400-G jack signal, on the other hand, disappears quickly at small tilt angles. It almost seems that the jack signal reappears at higher tilt angles, but these higher-field signals actually arise from the octahedron and correspond to approximately $\frac{3}{2}$ turns of the trajectory.

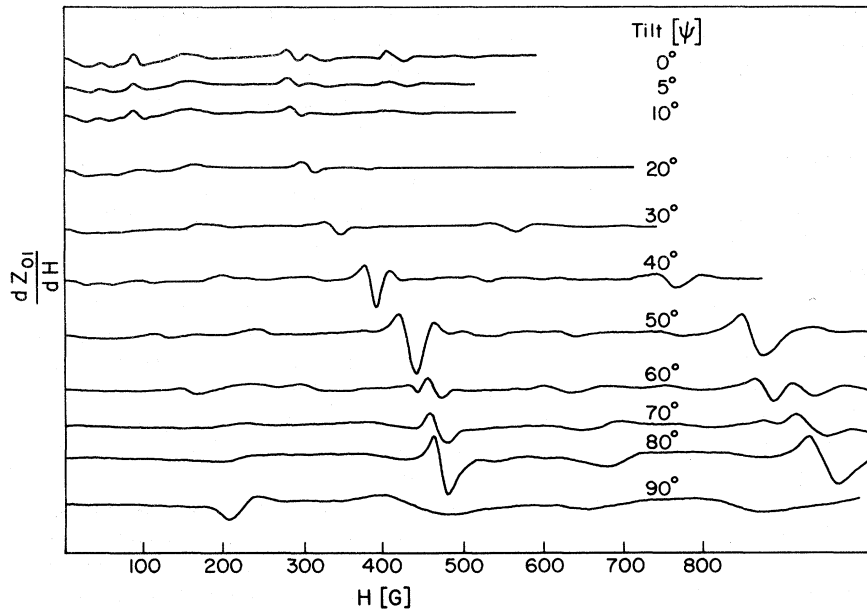


FIG. 5. Field derivative of the transmission coefficient at 4.2 K as a function of magnetic field for different tilt angles, as the field is rotated from $[1\bar{1}0]$ toward the $[110]$ plate normal.

In order to compare the experimental data and the ballistic RFSE model, an attempt was made to calculate all of the RFSE signals predicted for the model jack and octahedron sections of the tungsten FS for the field directions described above. The nature of the octahedron surface allows focused orbits producing large signals to exist; however, the jack surface produces mostly cutoff values of Hd_z involving very few electrons. Because observation of signals from these cutoff points is unlikely, attention has been devoted primarily to calculating the location of focused orbits.

The graph in Fig. 6 includes the onset fields of the Fig. 5 signals, and the calculated focused-orbit signal positions corresponding to fields satisfying $HD = (Hd_z)_{\text{ext}}$. Almost all of the well defined signals can be identified using the ballistic RFSE model and the RGGP FS model calculations. At zero tilt angle there is complete agreement between theory and experiment.

As the field is tilted, two curves evolve from the octahedron. As has already been noted, the upper octahedron signals in Fig. 6 come from orbits of roughly $\frac{3}{2}$ cyclotron period while the lower signals are from orbits of about $\frac{1}{2}$ period. The calculation indicates the rapid change in the position of the signal as a function of tilt angle, showing excellent agreement with experimental results for angles up to about 80° . The rapid disappearance of the jack two-ball orbit signal at $\psi \approx 10^\circ$ is due to the fact that at 10° none of the two-ball orbits are focused. The calculations indicate that the one-ball jack signal should exist for all tilt angles;

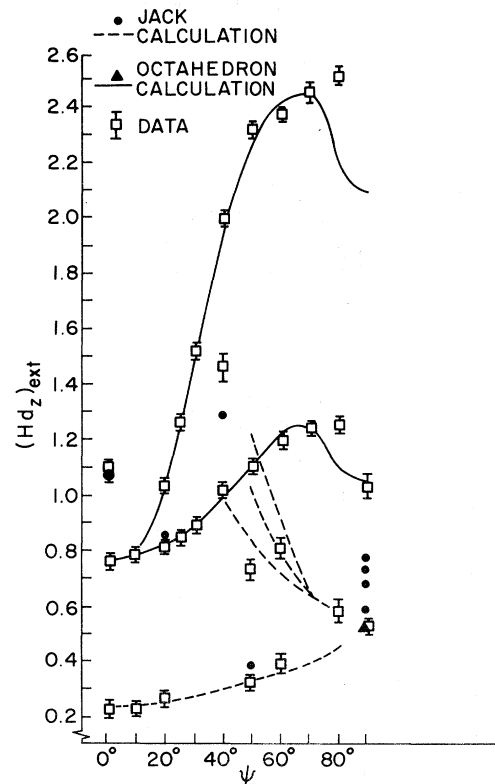


FIG. 6. Summary of observed onset fields and calculations for field directions between $[1\bar{1}0]$ ($\psi = 0$) and $[110]$ ($\psi = 90^\circ$). The isolated solid points represent calculated signals which exist only for very small ranges of tilt angle, and therefore do not evolve in any continuous manner as the tilt angle is changed.

although the data do not show a clear signal for all angles, the discernible signals agree with the calculations. Both GGP and RGGP models predict some jack signals between the jack one-ball orbit and the lower octahedron signals, though at slightly different values for the two models. While some signals are observed in this region, they appear to be of the periodic Gantmakher-Kaner type¹⁶ rather than primary RFSE signals as calculated, and may arise from an ellipsoid or a jack ball. The calculated signals may not be observable for two reasons. First, in both the GGP and RGGP models the several $(Hd_z)_{\text{ext}}$ which would produce signals occur near a cutoff of Hd_z , and might not be present using a more accurate FS model. Second, the calculated signals have a very long path length¹⁷ which severely limits the possibility of observing them.

Figure 7 shows some of the curves of Fig. 5 extended to higher magnetic fields where large signals of differing character are observed. The $\psi = 50^\circ$ curve has sharp peaks which decrease in amplitude with increasing field, a characteristic of RFSE signals, while the oscillations in the $\psi = 90^\circ$ curve are presumably Gantmakher-Kaner (GK) signals which grow with increasing magnetic field.¹⁸ The $\psi = 80^\circ$ curve is a mixture of both

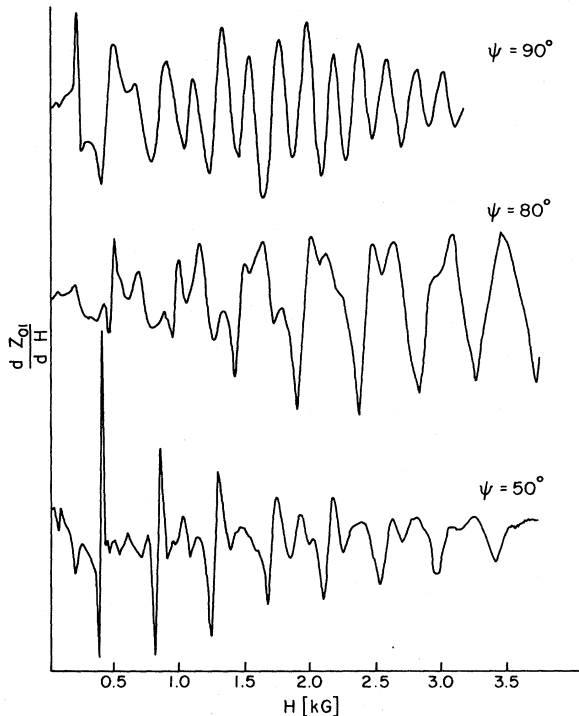


FIG. 7. Field derivative of transmission coefficient observed as a function of field, at fields extending beyond where the first-order RFSE signals occur.

types of signals, and can cause some confusion in the interpretation of RFSE results.¹⁹ These higher-field signals are observed at most tilt angles greater than 40° and their periods agree well with Sondheimer-magnetomorphic-effect data.^{12,17} Although it is not the intention of this paper to deal with GK signals in detail, some relations between RFSE and GK effects will be discussed in the following section.

Figure 8 shows the experimental results and related computer calculations for a tungsten sample with the magnetic field initially oriented along the $[1\bar{1}1]$ direction in the sample plane. The calculations were made only to identify the observed signals, not to predict all possible signals. The parallel-field signal ($\psi = 0$) and $Hd_z = 0.53$ originates from the octahedron, while the 0.25 and 0.46 are from a one-ball orbit and an octahedron-body orbit on the jack. A potential three-ball jack orbit signal is not clearly visible, possibly because the two-orbit chain signal from the octahedron (at 1.06) is rather large. The position of the octahedron signals as a function of tilt angle is very

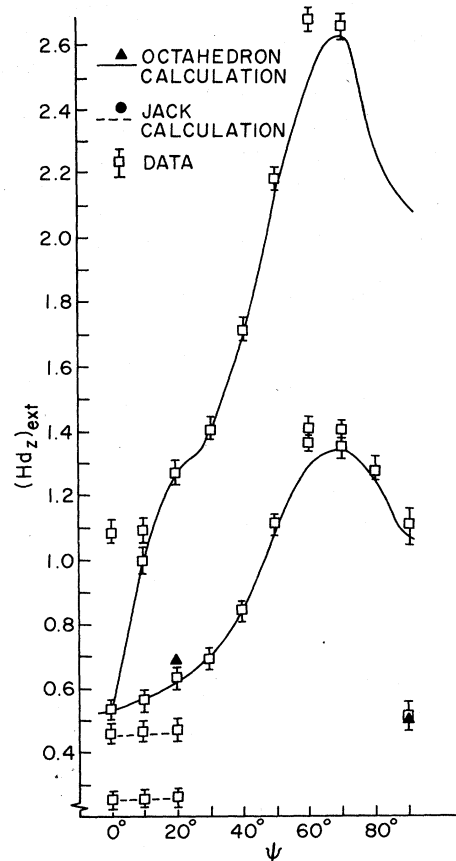


FIG. 8. Summary of experimental data and calculations for field directions between $[1\bar{1}1]$ ($\psi = 0$) and $[110]$ ($\psi = 90^\circ$).

similar to the data given earlier, although the second-order signal (corresponding to $\frac{3}{2}$ of a cyclotron period) separates from the first-order signal at a smaller tilt angle. The signals from the jack-body orbit exist to a moderate tilt angle, unlike the previous jack signals, and the jack one-ball orbit signal behaves as before. As in the previous data, the largest signals arise from the octahedron. The experimental agreement with the calculations is again quite good and allow identification of virtually all the observed signals; the greatest discrepancy between observed and calculated signal position is about 7%.

The calculations can also be used to identify the band of electrons producing the RFSE signals. While the parallel-field signal in the octahedron arises from "belly" orbits with $k_H = 0$, the focused orbits at large tilt angles have k_H up to 0.6 of the maximum k_H value for the octahedron. The electrons producing these tilted-field signals are thus from more localized sections of the FS than those producing the parallel-field signal and should therefore be useful for the measurement of electron scattering rates.

As shown in the calculations of Fig. 3, the octahedron section of the FS would seem to offer opportunities for observation of a cutoff or limiting-point signal; in other words, the slope of the curve at the cutoff of effective orbits is small enough to suggest that a sufficient number of electrons may be involved. We have not, however, observed such a signal even with the use of angle-modulation techniques which have enhanced these signals in potassium.²⁰

DISCUSSION

This study has shown that despite the moderate complexity of the tungsten FS, the parameterized FS model can be used in combination with the ballistic RFSE model to explain the RFSE in a tilted magnetic field. As previously noted, only the jack and octahedron sections of the FS have been considered although several signals from the jack are present, much of the observed data can be understood using only the octahedron surface. The ability of the calculations to explain the experimental data shows again the usefulness of the parametrized FS model; although it gives only an approximation of the true tungsten FS shape, the model has enabled several types of electron transport phenomena to be successfully interpreted.^{4,5,11,12} No effort has been made in this study to check systematically the details of the models for errors or to find possible corrections; for example, the positions of various parts of the RFSE lines have not been observed as a function of rf frequency in

order to locate exactly the onset of the signal. While there are small disagreements between the calculations and the observed data, the over-all agreement is considered very satisfactory.

The cutoff of effective orbits has not resulted in observable signals for either the jack or octahedron surfaces. This is not unreasonable given the small number of electrons involved, and the fact that the finite skin depth present in the experiments results in a less abrupt cutoff than that assumed by Peercy *et al.*² In addition, as shown in Ref. 1, a region of focused orbits usually exists near the cutoff value of Hd_z for a spherical FS; therefore, many of the signals observed in potassium which have been attributed to the cutoff of the effective orbits actually involve orbits which are focused. Although the calculated Hd_z curve for the tungsten octahedron is similar to that of potassium, in tungsten there are no focused orbits near the cutoff point and no signal is observed. Signals appearing near the cutoff point at small tilt angles are often called limiting-point signals, and the results for tungsten suggest that the observation of limiting-point signals may be restricted to metals with rather special FS characteristics.

Many experimenters have observed periodic signals in the surface impedance beyond the main RFSE resonance. At small tilt angles these signals seem clearly related to the RFSE, while at larger tilt angles they are similar to GK oscillations. The data presented in this paper suggest that it is not always possible to distinguish between the two effects.

GK signals are normally quasisinusoidal oscillations generated by electrons traveling on orbits which have extremal values of orbit pitch but no effective points. Although these signals were originally discussed for a magnetic field normal to a sample plate ($\psi = 90^\circ$),¹⁸ it is clear that they will also exist at other tilt angles. As already noted, the RFSE can produce narrow signals that appear periodic in field, due to electrons traveling in orbits of roughly $(2n + 1)/2$ cyclotron periods. In some situations, orbits which produce RFSE signals also meet the GK extremal pitch condition as shown below.

For most orbits d_z^n can be written as²¹

$$d_z^n = d_z^0 + nu(k_H) \sin\psi,$$

where d_z^n is the depth an electron penetrates into the metal as it moves between two effective points roughly $(2n + 1)/2$ cyclotron periods apart, d_z^0 is the corresponding distance when $n = 0$, and $u(k_H)$ is the orbit pitch. For small values of n , the extremal value of d_z^0 determines the orbit (k_H value) with extremal d_z^n . However, when $nu \sin\psi \gg d_z^0$, the extremal value of d_z^n occurs for the orbit which

has an extremal value of pitch. Thus, signals can be produced by orbits which satisfy *both* the RFSE conditions and the GK extremal-pitch condition. In some situations, as for a spherical FS, the extremal-pitch orbit has no effective points and can only be involved with GK oscillations. However, the calculations for the tungsten octahedron show that it is common for the orbit producing the d_z^1 extremal value to have a trajectory whose pitch is also extremal. Therefore, the period of these RFSE signals is essentially the same as the GK signal period.

CONCLUSION AND SUMMARY

We have shown that most of the tilted-field RFSE structure in tungsten is understandable in terms of the ballistic model of the RFSE combined with the parametrized tungsten FS model. The orbits that produce the tilted-field RFSE signals are not belly orbits ($k_H = 0$), as is common in the parallel-field case, but are orbits which are more localized

on the FS. These orbits are highly suited to the study of electron lifetimes on these FS sections. It has also been pointed out that under certain circumstances the period between the higher-order RFSE signals is the same as that of GK oscillations.

ACKNOWLEDGMENTS

I would like to thank B. Addis for preparing the tungsten samples used in this experiment and R. Cochran for his help with the computer calculations. I am particularly grateful to D. K. Wagner for allowing me to use his magnet system and transmission apparatus and for innumerable helpful conversations on this work. I also want to thank R. Bowers for his consultation and direction as my thesis adviser, B. W. Maxfield for suggestions made during the initial stages of the work, and B. W. Maxfield and J. W. Wilkins for critical readings of the manuscript.

*This work has been supported by the U. S. Atomic Energy Commission under Contract No. AT(11-1)-3150, Technical Report No. COO-3150-24.

†Current Address: Physics Department, University of Illinois, Urbana, Ill. 61801.

¹V. F. Gantmakher, in *Progress in Low Temperature Physics*, edited by C. J. Gorter (North-Holland, Amsterdam, 1967), p. 211.

²P. S. Peercy, W. M. Walsh, L. W. Rupp, and P. H. Schmidt, *Phys. Rev.* **171**, 713 (1968).

³See, for example, J. E. Bradfield and H. B. Coon, *Phys. Rev. B* **7**, 5072 (1973).

⁴R. F. Girvan, A. V. Gold, and R. A. Phillips, *J. Phys. Chem. Solids* **29**, 1485 (1968).

⁵S. W. Hui and J. H. Rayne, *J. Phys. Chem. Solids* **33**, 611 (1972).

⁶V. V. Bioko and V. A. Gasparov, *Zh. Eksp. Teor. Fiz.* **61**, 2362 (1972) [*Sov. Phys.—JETP* **34**, 1266 (1972)]; V. V. Bioko, V. F. Gantmakher, and V. A. Gasparov, *Zh. Eksp. Teor. Fiz.* **65**, 1219 (1973) [*Sov. Phys.—JETP*, March (1974)].

⁷W. M. Walsh, in *Solid State Physics Vol. 1: Electrons in Metals*, edited by J. F. Cochran and R. R. Haering (Gordon and Breach, New York, 1968).

⁸R. S. Thompson and A. Myers, *J. Phys. F* **3**, L64 (1973).

⁹For reviews of the RFSE and its use see Refs. 1, 7, and V. F. Gantmakher, *Rep. Prog. Phys.* **37**, 317 (1974).

¹⁰This paper uses notation similar to that of Peercy *et al.* (Ref. 2); therefore we refer to focused (extremal) and cutoff orbits. However, the authors of Ref. 2 incorrectly state that the signal associated with the cutoff of effective electron orbits in potassium is not associated with focusing. As shown by Gantmakher

(Ref. 1) and by careful analysis of Eq. (3) of Ref. 2, a section of focused orbits usually exists very near the effective orbit cutoff.

¹¹J. P. Kalejs and J. M. Perz, *Can. J. Phys.* **51**, 77 (1973).

¹²D. E. Soule and J. C. Abele, *Phys. Rev. Lett.* **23**, 1287 (1969); D. E. Soule and J. C. Abele, in *Low Temperature Physics LT-13*, edited by K. D. Timmerhaus, W. J. O'Sullivan, and E. F. Hammel (Plenum, New York, 1974).

¹³This method of calculation was recommended by D. K. Wagner and is described by Eugene Pacher, Ph.D. thesis (Cornell University, 1973) (unpublished).

¹⁴D. K. Wagner, *Rev. Sci. Instrum.* **45**, 621 (1974).

¹⁵D. K. Wagner and R. Cochran, *J. Low Temp. Phys.* **18**, 549 (1975).

¹⁶Periodic oscillations of the surface impedance have been described by Gantmakher and Kaner, and will be discussed later. See Ref. 18.

¹⁷D. R. Baer, Ph.D. thesis (Cornell University, 1974) (unpublished).

¹⁸V. F. Gantmakher and E. A. Kaner, *Zh. Eksp. Teor. Fiz.* **48**, 1572 (1965) [*Sov. Phys.—JETP* **21**, 1053 (1965)].

¹⁹There is some possibility that these oscillations could also be related to Doppler-shifted cyclotron resonance; see J. F. Carolan, in *Low Temperature Physics LT-13*, edited by K. D. Timmerhaus, W. J. O'Sullivan, and E. F. Hammel (Plenum, New York, 1974).

²⁰D. K. Wagner, R. C. Albers, and Manashi Roy, *Solid State Commun.* **15**, 1337 (1974).

²¹This form for d_z is similar, but not identical to Eq. (41) of Ref. 1.